ISSN 1087-6596, Glass Physics and Chemistry, 2021, Vol. 47, Suppl. 1, pp. S67–S74. © Pleiades Publishing, Ltd., 2021.

Synthesis of Iron Oxide Magnetic Nanoparticles and Their Effect on Growth, Productivity, and Quality of Tomato

A. S. Kovalenko[a,] *, A. M. Nikolaev[a], T. V. Khamova[a], O. R. Udalova[b], A. S. Zhuravleva[b], G. P. Kopitsa[a,c], A. A. Sinel'nikov[d], N. V. Tsvigun[e], Yu. V. Khomyakov[b], G. G. Panova[b], and O. A. Shilova[a]

[a] *Grebenshchikov Institute of Silicate Chemistry, Russian Academy of Sciences, St. Petersburg, 199034 Russia*

[b] *Agrophysical Research Institute, St. Petersburg, 195220 Russia*

[c] *Petersburg Nuclear Physics Institute, National Research Center "Kurchatov Institute," Gatchina, Leningrad oblast, 188300 Russia*

[d] *Voronezh State University, Voronezh, 394018 Russia*

[e] *Federal Scientific Research Centre "Crystallography and Photonics," Russian Academy of Sciences, Moscow, 119333 Russia*

**e-mail: anastasiya.bychk@mail.ru*

Received January 25, 2022; revised February 1, 2022; accepted February 8, 2022

Abstract—The influence of the structure, phase composition, textural and colloidal properties of magnetic iron oxides nanoparticles in the form of aqueous suspensions with a concentration of 0.001 and 0.01 mg/L on the growth, productivity of tomatoes and quality of its fruits after their foliar processing was shown. It was found that the maximum positive effect was observed during foliar treatment of tomato plants with aqueous suspensions of iron oxide samples with specific surface area (~52 and ~75 m^2/g), two-level hierarchical structure, hydrodynamic diameters (~150 and ~180 nm) in stable aqueous suspensions (the absolute value of the ζ-potential is ≈ 30 mV).

Keywords: iron oxide nanoparticles, water suspensions, foliar treatment, tomato

DOI: 10.1134/S1087659621070063

INTRODUCTION

In the last decade, iron oxide nanoparticles have been applied in many fields of science, including medicine and biology [1–3], where they are especially in demand due to their unique properties, such as biocompatibility, bioinertness, and superparamagnetism. It is known that iron is an essential microelement for the metabolism of most living objects, because the process of respiration and saturation of all cells of a living organism with oxygen is carried out due to it. These nanoparticles have entered the sphere of agricultural interests relatively recently [4–6], so the study of the interaction of iron oxide nanoparticles with a number of important agricultural crops is an urgent task of modern science at the intersection of chemistry and biology.

The purpose of present work is to describe the synthesis of iron oxide magnetic nanoparticles of various phase composition, structure and morphology, to study their properties and evaluate their effect on plant growth and development using the example of a tomato, its productivity and quality characteristics of fruits.

EXPERIMENTAL

Magnetic nanoparticles of iron oxides were synthesized by coprecipitation from aqueous solutions of iron(II) and iron(III) chlorides [7]. An aqueous solution of ammonium hydroxide acted as a precipitant. In order to study the effect of synthesis conditions on the phase composition, structure, morphology, texture, porosity and magnetic properties of iron oxides, the synthesis was carried out under various conditions, such as ultrasonic treatment (sample no. 87), long-term keeping of the precipitate in the mother liquor (sample no. 24), bubbling with argon (sample no. 17) and using oleic acid as a surfactant (sample no. 6).

The characterization of the obtained nanoparticles of iron oxides was carried out using XRD, TEM, low-temperature nitrogen adsorption, dynamic and electrophoretic light scattering, small angle polarized neutron scattering (SAPNS) and the method of nuclear magnetic resonance in a flowing liquid (nutation method).

X-ray powder diffraction (XRD) was used for phase identification. Measurements were carried out using Rigaku MiniFlex II diffractometer (CoK_a radiation, graphite monochromator, 2θ range 20–80 deg with a step of 0.05 and speed equal to 5 deg/min). Coherent Scattering Domain (CSD) length was calculated using 311 reflex with Debye–Scherrer formula.

The internal structure and shape of the nanoparticles were studied using high-resolution transmission electron microscopy (TEM) performed using a ZEISS Libra 120 transmission electron microscope.

The dynamic and electrophoretic light scattering method was used in order to determine the ζ-potential and hydrodynamic size of the particles in water. The measurements were performed using 90 Zeta Nano-Brook analyzer using the 0.1 g/L water ultrasonicated suspensions.

Measurements of the specific surface area of nanopowders were performed by low-temperature nitrogen adsorption using a QuantaChrome Nova 1200e analyzer. The samples were degassed at 150°C in a vacuum for 17 h prior to analysis. Based on the data obtained, the specific surface area SBET was calculated for the samples using the Brunauer–Emmett–Teller model (BET) and the seven points method within the relative pressure range of $P/P_0 = 0.07–0.25$ (where P_0 is the saturation pressure). The calculation of the pore size distribution was carried out on the basis of nitrogen isotherms using the Barrett–Joyner–Halenda (BJH) method.

The mesostructure, including the magnetic substructure of iron oxide powders, was studied by the SAPNS method, which allows the separation of nuclear and magnetic contributions to the observed small-angle neutron scattering. SAPNS measurements were carried out at the KWS-1 facility (FRM-II reactor, Garching, Germany). The KWS-1 installation is a classic small-angle diffractometer operating in a geometry close to a point. The experiment used a beam of polarized neutrons with an initial polarization of $P_0 \cong 0.95$ and a wavelength of $\lambda = 0.5$ nm with $\Delta\lambda/\lambda = 0.1$. The sample-detector distance SD = 8 m made it possible to measure the neutron scattering intensity in the range for the momentum transfer $0.08 < q = (4\pi/\lambda)\sin(\theta/2) < 1\ \text{nm}^{-1}$ (where θ is the scattering angle). Scattered neutrons were recorded by a two-dimensional scintillation position-sensitive detector based on ^{6}Li (128 × 128 cells with a spatial resolution of 5 × 5 mm^2).

Measurement of the magnetic properties of the powder was carried out by the method of nuclear magnetic resonance in a flowing liquid (nutation method) [8]. In series of vegetation experiments during growing plants under favorable controlled conditions of intensive light culture, the effect of foliar treating tomato plants with suspensions of iron oxide nanoparticles at concentrations of 0.001 and 0.01 mg/L on growth, plant productivity and product quality characteristics was evaluated. The objects of the study were the plants of the dwarf tomato variety Natasha bred by the Federal Scientific Center for Vegetable Growing. The plants were grown in plant growing light equipment [9, 10] with lifting light blocks located on a horizontal axis. High-pressure sodium lamps DNaZ-400 (Russia) were used as a light source, with the formation of irradiation in the usable area in the PAR (photosynthetically active radiation) range of 80–90 W/m^2. The duration of the light period was 16 h/day. Tomato plants were grown using thin-layer panoponics method with [11] the provision of nutrient solutions developed by the Agrophysical Research Institute. The air temperature was maintained within 22–24°C during the day and 18–20°C at night, relative air humidity 65–75%. The density of the cenosis was formed based on 1 m^2 of useful area of the plant growing light equipment: 20 plants. The repetition of plants in the experiment variant was 10. Vegetation experiments were repeated twice. Tomato plants were not formed, leaving all stepchildren on the stems. Foliar treatment of plants with aqueous suspensions was carried out three times during the formation of the 3rd, 5th, and 7th true leaves. Plants treated with water served as control. The collection of tomato fruits was carried out at the onset of consumer ripeness. Complete harvesting of plants was carried out on the 95th day. When harvesting, the number and weight of fruits of all collections, plant height, number of stems, wet and dry weight of leaves, stems and roots, percentage of dry matter, leaf surface area were taken into account [12]. Statistical data processing was performed using Excel 2010 and Statistica 8 software (Stat-Soft, USA). The average values of the studied parameters, confidence intervals, coefficients of variation were determined. The significance of differences between the variants was assessed by parametric (Student's t-test). Differences between the variants were considered significant at $p \leq 0.05$.

RESULTS AND DISCUSSION

The results obtained (Table 1) show that in all cases of synthesis, magnetic nanopowders of iron oxides were obtained. They possess phase composition of a solid solution of the magnetite-maghemite series with a different ratio of atoms of 2- and 3-valent iron, as evidenced by the values of the parameters of elemental cells (a) [13]. Also, the obtained nanopowders consist of particles of various sizes and shapes (from ~10 to ~20 nm), which is confirmed by the results of calculating the coherent scattering domains (CSD) lengths and the results of transmission electron microscopy (Fig. 1). The obtained materials have a sufficiently developed specific surface area (from ~52 to ~88 m^2/g). The results obtained by the method of small-angle scattering of polarized neutrons showed that the sample obtained using argon bubbling (no. 17) and the powder obtained by a similar method, but using oleic acid (no. 6), have a two-level hierarchical fractal structure, with a different characteristic scale of nuclear R_c and magnetic R_m correlations as well as the type of fractal aggregation for each of the levels (Table 2). At the

Table 1. Characteristics of the synthesized iron oxide nanopowders

Sample	a, Å	D_{CSD}, nm	S_{BET}, m^2/g	$M_{sp.rem}$, A m^2/kg	D, nm	ζ, mV
87	8.341(4)	13.8	80.9 ± 1.4	0.47	600	16 ± 4
17	8.355(4)	18.6	51.7 ± 1.1	1.06	155	30 ± 3
6	8.359(4)	11.5	75.0 ± 11.0	–	180	−30 ± 4
24	8.367(3)	13.4	87.5 ± 1.6	0.28	330	21 ± 3

a, unit cell parameter; D_{CSD}, coherent scattering domain length; S_{BET}, specific surface area; $M_{sp.rem}$, specific remanence; D, hydrodynamic diameter; ζ, zeta potential.

Table 2. Parameters of the nuclear and magnetic structure of the iron oxide nanopowders obtained using argon bubbling

Sample	D_{S1}	R_{c1}, nm	R_{m1}, nm	D_{M2}	R_{c2} (R_{m2}) nm
17	2.03 ± 0.05	6.8 ± 1.3	11.2 ± 1.2	2.33 ± 0.02	>45
6	2.55 ± 0.06	5.7 ± 0.4	4.7 ± 0.5	2.41 ± 0.02	

D_{S1}, dimension of the surface fractal of the 1st structural level; R_{c1}, the upper limit of self-similarity of the surface fractal of the 1st structural level; R_{m1}, characteristic radius of the magnetic correlations of the 1st structural level; D_{M2}, dimension of the mass fractal of the 2-nd structural level; R_{c2}, the upper limit of self-similarity of the mass fractal of the 2nd structural level; R_{m2}, characteristic radius of the magnetic correlations of the 2nd structural level.

same time, samples obtained under ultrasonic treatment (no. 87) and with prolonged exposure of the precipitate in the mother liquor (no. 24) consist of randomly oriented non-spherical magnetic inhomogeneities of the fibrillar type (Table 3). The study of the magnetic properties of the obtained nanopowders showed that all samples are magnetically soft materials, however, the sample no. 17 has the highest remanent magnetization (1.06 A m^2/kg), alongside with the smallest value of the specific surface area, the highest CSD length and characteristic radius R_{m1} of the magnetic correlations and also characterized by a two-level hierarchical organization of the structure.

Table 3. Parameters of the nuclear and magnetic structure of the iron oxide nanopowders obtained under ultrasonic treatment

Sample	D_S	R_c, nm	R_m, nm
87	2.05 ± 0.05	4.7 ± 0.5	6.0 ± 0.7
24	2.30 ± 0.06	5.9 ± 0.7	6.7 ± 0.7

D_{S1}, dimension of the surface fractal of the non-spherical inhomogeneities of the fibrillar type; R_{c1}, radius of the non-spherical inhomogeneities of the fibrillar type, R_{m1}, characteristic radius of the magnetic correlations of the non-spherical inhomogeneities of the fibrillar type.

Based on the synthesized magnetic nanoparticles of iron oxides, aqueous suspensions with a concentration of 0.001 and 0.01 mg/L were created, in which colloidal properties (ζ-potential and hydrodynamic diameter) were studied by dynamic and electrophoretic light scattering. Samples synthesized by bubbling with argon (no. 17) and using oleic acid (no. 6) had the smallest hydrodynamic diameters in aqueous suspensions, ~150 and ~180 nm, respectively, and formed stable aqueous suspensions, which was confirmed by absolute the value of ζ-potentials equal to 30 mV. At the same time, the sample synthesized using oleic acid had a negative value of the ζ-potential in an aqueous medium, in contrast to other samples.

The resulting aqueous suspensions at predetermined plant-friendly concentrations of 0.001 and 0.01 mg/L were used for foliar treatment of tomato plants.

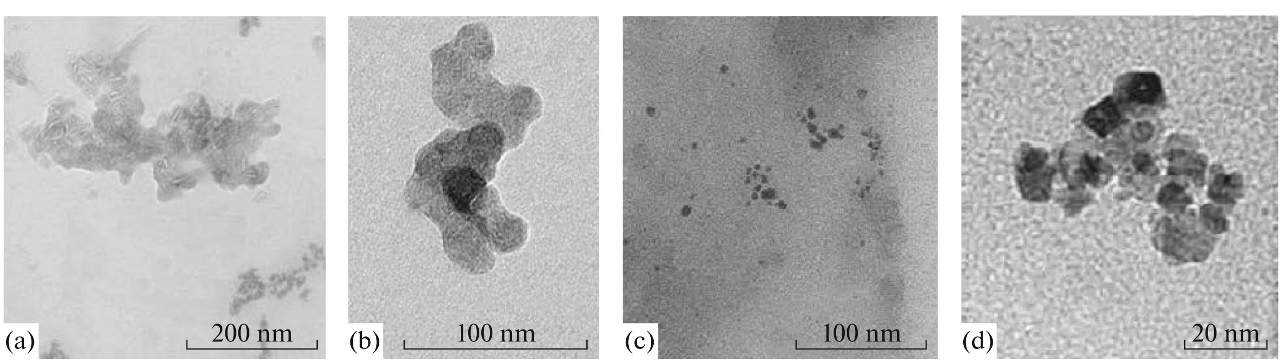

Fig. 1. TEM images of the iron oxide nanoparticles: (a) sample no. 24; (b) sample no. 87; (c) sample no. 17; (d) sample no. 6.

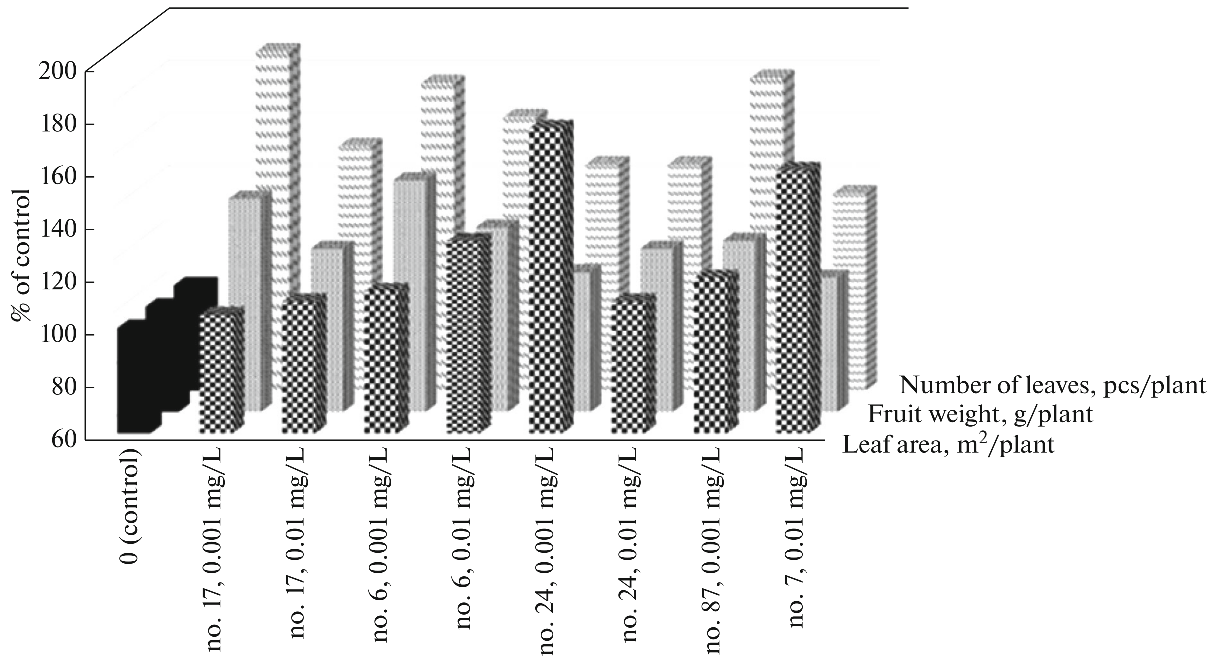

Fig. 2. Influence of foliar treatment of tomato plants with suspensions of iron oxide nanoparticles of various compositions on its productivity and leaf surface area.

In the treated tomato plants, a trend or a significant increase in the number (by 11–48%) and weight of fruits (by 35–89%) was noted in all the studied variants of the experiment (Fig. 2 and Table 4).

The increase in the productivity of tomato plants under the influence of the test substances is due to an increase in the area of the assimilating surface of the leaves, the mass of root systems, and, consequently, the total area of absorption of nutrients, as well as due to the accumulation and redistribution of nutrients and plastic substances into the generative organs. Thus, in the variants with foliar treatment with the test substances, a trend or a significant increase in the leaf surface area (by 10–76%) was noted in comparison with the control (Fig. 2 and Table 4). There was also an

Table 4. The effect of foliar tomato treatment with suspensions of iron oxide nanoparticles of various compositions on plant productivity and leaf surface area

Aqueous suspension of the substance	Number of fruits/plant		Fruit weight/plant		Leaf area	
	PCS	% of control	g	% of control	m^2/plant	% of control
0 (control)	17.8 ± 3.2	100	220 ± 28	100	0.21 ± 0.02	100
no. 17 0.001 mg/L	33.6* ± 4.1	189*	311* ± 19	141*	0.22 ± 0.02	105
no. 17 0.01 mg/L	27.2* ± 6.1	153*	269* ± 20	122*	0.23 ± 0.02	110
no. 6 0.001 mg/L	31.6* ± 6.3	177*	325* ± 49	148*	0.24 ± 0.03	114
no. 6 0.01 mg/L	29.2* ± 6.3	164*	286* ± 37	130*	0.28* ± 0.03	133*
no. 24 0.001 mg/L	26.0* ± 5.9	146*	249* ± 45	113	0.37* ± 0.04	176*
no. 24 0.01 mg/L	26.0* ± 2.7	146*	268* ± 19	122*	0.23 ± 0.02	110
no. 87 0.001 mg/L	31.8* ± 6.8	179*	274* ± 26	125*	0.25 ± 0.03	119
no. 87 0.01 mg/L	24.0* ± 2.9	135*	245 ± 22	111	0.34* ± 0.04	160*

* The value significantly differs from the control at the 5% significance level.

Table 5. The effect of tomato treatment with suspensions of iron oxide nanoparticles of various compositions on plant growth indicators

Aqueous suspension of the substance	High	Number of stems	Leaves						Stems					
			raw mass		dry mass		dry matter		raw mass		dry mass		dry matter	
			g/plant	% of control	g/plant	% of control	%	% of control	g/plant	% of control	g/plant	% of control	%	% of control
0 (control)	22.8 ± 2.6	8.6 ± 0.8	52 ± 4.9	100	6.4 ± 0.7	100	12.3 ± 0.6	100	42.0 ± 3.0	100	5.0 ± 0.6	100	11.8 ± 0.5	100
no. 17 0.001 mg/L	20.4 ± 1.1	8.6 ± 1.1	58 ± 5.2	112	6.6 ± 0.8	103	11.3 ± 0.5	92	42.0 ± 9.7	100	4.6 ± 0.6	92	10.9 ± 0.6	92
no. 17 0.01 mg/L	23.0 ± 4.1	8.8 ± 1.2	68* ± 5.4	131*	7.8* ± 0.7	122*	11.5 ± 0.6	93	46.4 ± 9.3	110	5.1 ± 0.7	102	11.1 ± 0.5	94
no. 6 0.001 mg/L	21.6 ± 1.9	8.8 ± 0.4	57 ± 5.9	110	6.9 ± 0.9	108	12.1 ± 0.5	98	43.0 ± 6.1	102	4.7 ± 0.7	94	10.9 ± 0.5	92
no. 6 0.01 mg/L	22.4 ± 3.3	8.8 ± 0.8	64* ± 4.7	123*	7.1 ± 0.6	110	11.2 ± 0.6	90	41.2 ± 6.4	98	4.4 ± 0.7	88	10.8 ± 0.6	92
no. 24 0.001 mg/L	24.2 ± 2.3	9.8 ± 1.2	94* ± 6.3	181*	11.8* ± 1.0	184*	12.6 ± 0.5	102	46.4 ± 5.8	110	5.3 ± 0.6	106	11.4 ± 0.5	97
no. 24 0.01 mg/L	22.4 ± 1.6	9.6 ± 1.8	63* ± 5.9	121*	6.7 ± 0.9	105	10.3* ± 0.5	84*	35.6 ± 4.7	85	4.1* ± 0.3	82*	11.4 ± 0.4	97
no. 87 0.001 mg/L	22.2 ± 1.8	9.8 ± 1.7	71* ± 6.0	137*	9.8* ± 0.6	153*	13.8* ± 0.6	112*	40.8 ± 7.0	97	4.8 ± 0.8	96	11.7 ± 0.6	99
no. 87 0.01 mg/L	23.8 ± 3.4	9.2 ± 0.8	91* ± 7.0	182*	11.1* ± 1.2	173*	12.2 ± 0.5	99	40.5 ± 8.7	97	4.7 ± 0.7	97	11.6 ± 0.5	98

* The value significantly differs from the control at the 5% significance level.

Table 6. Quality indicators of tomato fruits after foliar treatment of plants with suspensions of iron oxide nanoparticles of various compositions

Chemical composition indicators	Aqueous suspension of the substance								
	0 (control)	no. 17 0.001 mg/L	no. 17 0.01 mg/L	no. 6 0.001 mg/L	no. 6 0.01 mg/L	no. 24 0.001 mg/L	no. 24 0.01 mg/L	no. 87 0.001 mg/L	no. 87 0.01 mg/L
Humidity, %	94.2	94.4	94.1	94.4	94.7	93.7	93.8	93.9	93.5
Dry matter, %	5.8	5.6	5.9	5.6	5.3	6.3	6.2	6.1	6.5*
Raw ash, %	12.33	12.26	12.83	12.63	12.63	12.16	12.58	12.35	12.65
Nitrogen, % absolutely dry substance	3.85	3.89	3.97	3.91	4.08	4.00	4.05	4.23	3.89
Phosphorus, % absolutely dry substance	0.67	0.65	0.68	0.64	0.66	0.68	0.64	0.65	0.62
Potassium, % absolutely dry substance	6.24	6.29	6.36	6.17	6.23	6.40	6.36	6.22	6.28
Calcium, % absolutely dry substance	0.75	0.87*	0.86*	0.71	0.77	0.74	0.72	0.71	0.77
Magnesium, %. absolutely dry substance	0.227	0.259*	0.258*	0.242	0.316*	0.227	0.239	0.231	0.246
Sum of sugars, % absolutely dry substance	10.97	11.20	11.18	11.97	11.24	11.53	11.31	11.65	12.09
Vitamin C, mg/100 g substance of natural moisture	16.4	19.1*	24.2*	19.8*	24.9*	28.6*	21.1*	30.4*	30.8*
Nitrates, mg/kg substance of natural moisture	124.0	126.0	118.0	139.0	136.0	124.0	110.0	105.0*	116.0
Copper content, mg/kg absolutely dry substance	0.275	0.243*	0.373*	0.250	0.421*	0.075*	0.072*	0.133*	0.108*
Zinc content, mg/kg absolutely dry substance	18.9	19.6	19.8	18.5	18.7	17.6	16.8	17.7	17.5
Iron content, mg/kg absolutely dry substance	29.7	37.5*	40.2*	52.2*	74.5*	39.8*	44.4*	36.9*	41.7*
Manganese content, mg/kg absolutely dry substance	10.3	10.27	10.2	14.8*	14.2*	10.33	10.59	10.57	0.38*

* The value significantly differs from the control at the 5% significance level.

increase in the raw (by 10–82%) and dry (by 3–84%) mass of the tomato plants leaves (Table 5).

At the same time, in the variants of foliar treatment of plants with suspensions of iron oxide nanoparticles, the quality of tomato fruits increased, as evidenced by an increase in the content of sugars (by 2–10%) and vitamin C (by 16–87%), as well as most mineral elements (Table 6). The nitrate content in tomato fruits had a predominant tendency or significantly lower values (by 5–15%) compared to that in control plants, which indicates an increase in their safety and compliance with the sanitary and hygienic requirements of the Russian Federation.

The most significantly characterized effect on the productivity of tomato plants during the formation of fruits with higher quality characteristics compared to the control was provided by foliar treatment with suspensions of samples nos. 17 or 6 at concentrations of 0.001 and 0.01 mg/L, as well as no. 87—at concentrations of 0.001 mg/L, no. 24—at concentrations of 0.01 mg/L. At the same time, the maximum values of productivity indicators were noted in the variants with treatment with suspensions of samples nos. 17 or 6 at a concentration of 0.001 mg/L. This is most likely due to the unique set of properties of these samples that distinguish them from other synthesized materials, namely, the smallest value of specific surface areas (~52 and ~75 m^2/g, respectively), two-level hierarchical structure, the smallest size of hydrodynamic diameters (~150 and ~180 nm), stability of suspensions based on them ($|\zeta| \approx 30$ mV).

CONCLUSION

Thus, we can conclude that the synthesis conditions have a significant effect on all the studied properties of iron oxide nanopowders: phase composition, structure, morphology, texture, magnetic and colloidal properties. It should be noted that bubbling with argon during synthesis promotes a decrease in the specific surface area (both with oleic acid and without the use of surfactants) and leads to structure ordering, an increase in magnetic properties, and better stabilization of particles in aqueous suspensions. Ultrasonic exposure promotes the oxidation of freshly obtained magnetite nanoparticles and their almost complete transformation into maghemite, in addition, it leads to agglomeration of particles with random orientation and, as a result, to large values of the hydrodynamic diameter of particles in aqueous suspensions, which are not sufficiently stable, judging by the value of the ζ-potential (~16 mV). Long-term ageing of the precipitate in the mother liquor leads to the production of iron oxide nanoparticles with a phase composition closest to that of magnetite and contributes to an increase in the specific surface area to ~88 m^2/g. The use of oleic acid during synthesis leads to a decrease in the specific surface area of iron oxide nanopowder to ~75 m^2/g, possibly due to its partial filling of pores, which leads to surface smoothing.

Foliar treatments of tomato plants with obtained aqueous suspensions based on synthesized iron oxide nanoparticles had a positive effect on plants, expressed in an increase in their growth rates, productivity, improvement of the quality and safety of the formed plant products, namely: an increase in the content of sugars, vitamin C, and macro- and microelements, predominantly reducing the content of nitrates.

The results obtained show the promise of further studies of the properties of magnetic iron oxide nanoparticles and the mechanisms of their influence on cultivated plants for the creation and use in crop production of new highly effective environmentally friendly nanopreparations.

ACKNOWLEDGMENTS

XRD studies were carried out using equipment of the Center for Collective Usage of the Federal Research Center “Crystallography and Photonics” of the Russian Academy of Sciences (Moscow, Russia) with the support of the RF Ministry of Science and Higher Education.

CONFLICT OF INTEREST

The authors declare that they have no conflicts of interest.

REFERENCES

1. Uchechukwu, S.E., Blessing, N.E., Samson, O.A., and Fabian, I.E., Iron oxide nanoparticles in biological systems: Antibacterial and toxicology perspective, *JCIS Open*, 2021, vol. 4, 100027.
2. Roghayyeh, B., Mehrdad, A., Jafar, S., and Mahdi, R., Were magnetic materials useful in cancer therapy?, *Biomed. Pharmacother.*, 2021, vol. 144, 112321.
3. Cotin, G., Piant, S., Mertz, D., Felder-Flesch, D., and Begin-Colin, S., Iron oxide nanoparticles for biomedical applications: Synthesis, functionalization, and application, in *Metal Oxides*, *Iron Oxide Nanoparticles for Biomedical Applications*, Mahmoudi, M. and Laurent, S., Eds., Amsterdam: Elsevier, 2018, Chap. 2, pp. 43–88
4. Panova, G.G., Shilova, O.A., Nikolaev, A.M., Kovalenko, A.S., Udalova, O.R., Anikina, L.M., Zhuravleva, A.S., Khomyakov, Yu.V., Vertebnyi, V.E., and Dubovitskaya, V.E., On the impact of iron oxide nanoparticles on plants in the vegetative period of development, *Agrofizika*, 2019, no. 3, pp. 40–50.
5. Tombuloglu, H., Slimani, Ya., Tombuloglu, G., Almessiere, M., and Baykal, A., Uptake and translocation of magnetite (Fe_3O_4) nanoparticles and its impact on photosynthetic genes in barley (*Hordeum vulgare* L.), *Chemosphere*, 2019, vol. 226, pp. 110–122.
6. Lu, K., Shen, D., Liu, X., Dong, Sh., Jing, X., Wu, W., Tong, Ya., Gao, Sh., and Mao, L., Uptake of iron oxide nanoparticles inhibits the photosynthesis of the wheat after foliar exposure, *Chemosphere*, 2020, vol. 259, 127445.
7. Shilova, O.A., Nikolaev, A.M., Kovalenko, A.S., Sinel’nikov, A.A., Yorov, Kh.E., Tsvigun, N.V., Volkov, V.V., Khamova, T.V., Panova, G.G., and Kopitsa, G.P.,

Aqueous chemical synthesis of iron oxides magnetic nanoparticles of different morphology and mesostructure, *Ceram. Int.*, 2021, vol. 47, no. 20, pp. 28866–28873.

8. Zhernovoy, A.I., Naumov, V.N., and Rudakov, Yu.R., Paramagnetic nanoglobules dispersion curve definition via magnetization and magnetizable field using NMR method, *Nauch. Priborostr.*, 2009, vol. 19, no. 3, pp. 57–61.
9. Zheltov, Yu.I. and Panova, G.G., A device for growing plants, RF Patent 108705, 2011.
10. Panova, G.G., Chernousov, I.N., Alexandrov, A.V., and Zheltov, Yu.I., A device for growing plants, RF Patent 137446, 2014.
11. Chernousov, I.N., Panova, G.G., Udalova, O.R., and Alexandrov, A.V., Phytotechnical complex for growing plants, RF Patent 189309, 2019.
12. Tret'yakov, N.N., *Praktikum po fiziologii rastenii* (Educational Aid on Plant Physiology), Moscow: Agropromizdat, 1990.
13. Shilova, O.A., Nikolaev, A.M., Kovalenko, A.S., Sinel'nikov, A.A., Kopitsa, G.P., and Baranchikov, A.E., Synthesis of magnetic nanopowders of iron oxide: Magnetite and maghemite, *Russ. J. Inorg. Chem.*, 2020, vol. 65, no. 3, pp. 426–430.